Journal of Sol-Gel Science and Technology 26, 267–271, 2003

X-Ray Absorption and Diffraction Studies of Pr^{3+}, Tb^{3+} and Er^{3+}-Activated Silica Gels

F. ROCCA*, C. ARMELLINI AND M. FERRARI
IFN-Istituto di Fotonica e Nanotecnologie del CNR Sezione CeFSA di Trento, via Sommarive 18, I-38050 POVO Trento, Italy
rocca@science.unitn.it

G. DALBA
Dipartimento di Fisica and INFM, Università di Trento, via Sommarive 14, I-38050 POVO Trento, Italy

N. DIAB
Department of Physics, Faculty of Science, University of ASSIUT, Egypt

A. KUZMIN
Institute of Solid State Physics, University of Latvia, Kengaraga Street 8, LV-1063 RIGA, Latvia

F. MONTI
Dipartimento di Informatica, Facoltà di Scienze, Università di Verona, Strada le Grazie, I-37134 VERONA, Italy

Abstract. Rare-earth (Pr^{3+}, Tb^{3+}, Er^{3+}) doped silica xerogels were studied by x-ray absorption spectroscopy and x-ray diffraction. A change of the local environment around rare-earth ions upon xerogel densification at 900–950°C and co-doping with aluminum ions was determined from the rare-earths L_3-edge EXAFS signals. The densification process induces a decrease of the coordination number and a compression and deformation of the first coordination shell, composed of oxygen atoms. The second coordination shell, composed of silicon and/or aluminum ions, also experiences some modification, which is attributed mainly to a shortening of the shell radius. No evidence of clustering of rare-earth ions upon densification was observed. X-ray diffraction data on Tb-doped gels confirm the EXAFS results.

Keywords: EXAFS, XRD, rare-earth ions, xerogels

1. Introduction

Silica-based sol-gel glasses activated by rare-earth (RE) ions are attractive materials for integrated optics devices as solid state lasers and fiber amplifiers for optical signals. The optical properties of these materials can be tuned [1–4] by changing the densification process and by varying the type and the concentration of the RE ions or by co-doping with other ions. To have a strong amplification effect, the concentration of the RE ions in the glass should be as high as possible. However, at high level of doping, a clustering of the RE ions [5, 6] occurs that results in a quenching of the fluorescence intensity and a shortening of the fluorescence lifetimes. This limits the RE concentration to a few percent molar. In order to optimize the performance of the RE-doped glasses, detailed information on the local structure around the optically active ions is required [5–12].

*To whom all correspondence should be addressed.

In this work, a comparative study of Pr^{3+}, Tb^{3+} and Er^{3+}-doped silica gels by two complementary structural techniques, the extended x-ray absorption fine structure (EXAFS) spectroscopy and x-ray diffraction (XRD), is presented. EXAFS was carried out at the RE L_3-edge. The influence of the RE ion type and the RE concentration on the local environment around the RE ions in wet and high-temperature treated silica xerogels will be discussed.

2. Experimental and Data Analysis

Silica xerogel samples were prepared via hydrolysis and condensation of the rare-earth nitrate hydrate solutions in tetramethylorthosilicate (TMOS), methanol and de-ionized water in the presence of nitric acid as a catalyst [5–7]. The concentration of the Pr^{3+}, Tb^{3+} and Er^{3+} ions was in the range from 400 to 40000 ppm. Besides, some Er^{3+}-doped xerogels were also co-doped with aluminum ions at two Er/Al molar ratios (1:6 and 1:9). Freshly prepared wet xerogels will be referred to as non-treated (NT), the ones densified at 900–950°C as high-temperature treated (HT).

EXAFS measurements [5–7] were performed at room temperature (RT) in fluorescence mode at the Pr^{3+}, Tb^{3+} and Er^{3+} L_3-edges at the BM8 GILDA CRG beamline of ESRF (Grenoble, France). As reference compounds water solutions of RE nitrate hydrates, crystalline $PrVO_4$, $TbVO_4$, $ErVO_4$, Er_2O_3, and $Er(OH_2)_9(CF_3SO_3)_3$ were also measured in transmission mode. XRD measurements were made at RT both at the GILDA beamline and by a diffractometer equipped with conventional x-ray tubes in our Laboratory.

The EXAFS signals were analysed by the EDA code [13] using the procedure described in refs. [13] and [14]. Theoretical amplitude and phase shift functions used in the EXAFS modeling were calculated by the FEFF6 code [15], and checked with reference compounds [5–7]. The Fourier transforms of the experimental EXAFS signals are shown in Fig. 1. The local environment around RE ions in the xerogels was reconstructed using two approaches: regularization-like method and the Gaussian-type three-shells (RE–O, RE–Si/Al, RE–O) model. The first method allowed us to determine accurate first shell RE–O pair distribution functions (PDFs) and indicated slight asymmetry of the PDFs. The second method allowed us to obtain information also on the second RE–Si/Al coordination shells (Table 1).

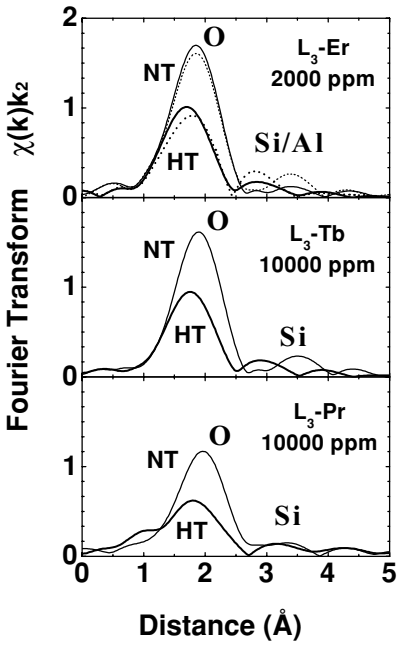

Figure 1. Fourier transforms of the rare-earth L_3-edge EXAFS signals in NT (solid lines) and HT (bold lines) silica xerogels. Dashed lines correspond to Er-doped xerogels co-doped with aluminum (Er:Al = 1:9). Positions of the oxygen and silicon/aluminum shells are indicated.

The XRD technique was used to obtain complementary information on the total radial distribution functions (RDFs) [12]. RDFs correspond to a sum of the PDFs as Si–O, O–O, Si–Si, RE–O, RE–Si and RE–RE. To enhance the contribution of RE ions, the difference between the RDFs for RE-doped and undoped xerogels can be calculated. Figure 2 shows an example of such analysis for the Tb^{3+}-doped xerogels.

3. Results and Discussion

A comparative analysis of the EXAFS results for Pr^{3+}, Tb^{3+} and Er^{3+}-doped xerogels, obtained in this and our previous works [5–7], allows us to follow a variation of the short range order around RE ions as a function of the thermal treatment, the doping concentration and the co-doping with aluminum ions.

In NT xerogels, the first coordination shell of RE ions is well defined and consists of 7–8 oxygen atoms. Both the shell radius R(RE–O) and the mean-squared relative displacements (MSRDs) σ^2(RE–O) increase by going from small and more electropositive Er^{3+} ion to large and more electronegative Pr^{3+} ion (Table 1). The difference in the RE–O distances agrees very

Table 1. Summary of local environment around rare-earth (RE) ions in non-treated (NT) and high-temperature (900–950°C) treated (HT) silica xerogels from EXAFS data.

	Pr^{3+}		Tb^{3+}		Er^{3+}	
	NT	HT	NT	HT	NT	HT
	First coordination shell, RE—O					
N (±0.7)	8	6.2	7–7.5	5.9–6.3	7–7.8	6–6.5
R (±0.02 Å)	2.53	2.47	2.42	2.35	2.39	2.32
σ^2(±0.004 Å^2)	0.012	0.023	0.010	0.020	0.007	0.0019
	Second coordination shell, RE—Si					
N (±1)	3	2	1–3	2–3	3–5	2–4
R (±0.04 Å)	4.19	3.96	4.10	3.70	3.95	3.14
σ^2 (±0.02 Å^2)	0.01	0.007	0.005	0.02	0.01–0.04	0.01–0.03
α (±4°)	180	147	180	138	162	104

Reported data are averaged values from available measurements on samples having RE ion content between 1000 and 10000 ppm. N is the coordination number, R is the interatomic distance (RE—O or RE—Si), σ^2 is the MSRD and α is the RE—O—Si angle.

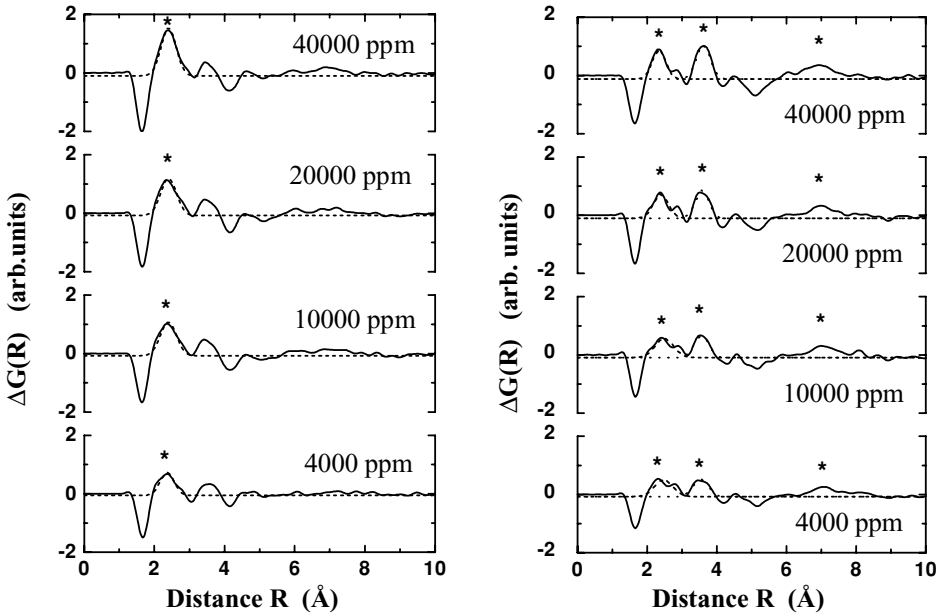

Figure 2. The difference $\Delta G(r)$ between RDFs, determined by XRD, for Tb-doped and undoped xerogels as a function of Tb-doping: non-treated xerogels on the left panel, HT (950°C) treated xerogels on the right panel. The peaks, attributed to Tb—O, Tb—Si and Tb—Tb contributions, are labeled by asterisks. The Gaussian fits of the peaks are shown by dashed lines. Note that the negative peak at ∼1.6 Å indicates structural modifications of the silica network due to Tb-doping.

well with the difference in the corresponding RE ionic radii ($R_{ion}(Er^{3+}) = 0.88$ Å, $R_{ion}(Tb^{3+}) = 0.92$ Å and $R_{ion}(Pr^{3+}) = 1.01$ Å). We did not observe significant dependence of the local environment on the RE concentration in the NT xerogels.

On the contrary, the co-doping with aluminum strongly affects mainly the RE second coordination shell. In particular, with increasing the aluminum content in the NT Er^{3+}-doped xerogels, the second shell radius increases from 3.95 Å to 4.12 Å, for a Er:Al

molar ratio ranging from 0 to 1:9. At the same time, the MSRD value decreases of ∼0.01 Å^2 indicating a narrower distance distribution. This suggests a preferential bonding of the Er^{3+} ions to aluminum ions with respect to silicon.

A big change of the local environment around RE ions occurs upon densification of the xerogels at 900–950°C. The RDFs, reconstructed from the EXAFS data, reveal a decrease of the first shell coordination number, a shortening of the RE—O distances and a broadening of the first shell with respect to the NT samples (Table 1). Note that the difference between RE—O distances for the three RE ions resembles again the difference in the ionic radii. The first shell RDF becomes also slightly asymmetric with a tail at longer distances. The asymmetry is more evidenced in $Pr^{3+}$and Tb^{3+} -doped xerogels than for Er^{3+}-doped xerogels, suggesting a stronger Er—O bond. A big contraction of the interatomic distances was also found in the second coordination shell.

The co-doping with aluminum has a significant impact on the local structure of RE ions in densified xerogels too. In the presence of aluminum, the first shell Er—O distance increases of about 0.02–0.05, and the second shell radius, corresponding to the Er—Si/Al distances, increases from 3.14 to 3.21 Å. At the same time, the Er—Al distances have the MSRD twice smaller than Er—Si. The EXAFS results do not show any evidence of a clustering for RE ions after densification: the short range RE—RE coordination is absent or not detectable in the present experiments.

The knowledge of the RE—O and RE—Si/Al distances allows us to estimate the value and the variation of the RE—O—Si/Al angles. We assume the Si—O distance equal to 1.62 Å and the Al—O distances equal to 1.76 Å for tetrahedral [AlO_4] and 1.94 Å for octahedral [AlO_6] coordinations, respectively. In such a case, the average RE—O—Si/Al angles change upon densification from 180° to 147° for Pr—O—Si; from 180° to 138° for Tb—O—Si; from 162° to 104° for Er—O—Si and from 164° to 103° for Er—O—AlO_3 (or from 143° to 98° for Er—O—AlO_5).

The influence of doping on the XRD spectra and the relative differential correlation functions, $G(r)$, is more difficult to be analysed, because of the very reduced RE concentrations. So, XRD data seem less sensitive than EXAFS. However, differential analysis of XRD, carried out by subtracting the spectrum of the undoped sol gel from the spectra of the Tb-doped samples with increasing RE content (Fig. 2), allows us to identify the pair correlations due to the presence of terbium ions and also to see some modifications induced on the silica network. The Tb—O contribution is already well visible in the NT xerogels, being in good agreement with the EXAFS data. In densified xerogels, two additional contributions becomes also visible at ∼3.6 Å and ∼7 Å. We attribute them to Tb—Si and Tb—Tb correlations, respectively. Note that the band at ∼7 Å is so broad than it was not detected by EXAFS. The last noticeable result is the negative peak at ∼1.6 Å visible in both NT and HT xerogels. It is related to the difference in the Si—O bonding in undoped and doped xerogels.

4. Conclusions

Local environment around Pr^{3+}, Tb^{3+} and Er^{3+} ions in NT and densified silica xerogels has been reconstructed from the EXAFS data by two different methods of analysis, leading to similar conclusions. The use of scattering amplitude and phase shift functions, tested on several crystalline reference compounds, and comparative analysis with XRD measurements provide us a high degree of confidence in the obtained results.

The short range order around rare-earth ions was found to be strongly affected by the thermal treatment, whereas no significant dependence on RE ions concentration was observed in the doping range from 400 to 40000 ppm. The densification induces a decreasing of the coordination number and a shortening and deformation of the RE—O coordination shell. EXAFS does not show any evidence of clustering of RE ions upon densification, since the short range RE—RE coordination is absent or not detectable in the present experiments even at the highest RE-doping. On the other hand, the effects of aluminum co-doping are clearly monitored in the first and second coordination shells. The absence of clustering is confirmed by the XRD measurements. The general trends observed are consistent with a variation of the RE ions size and electropositivity.

Acknowledgments

A.K. wish to thank the Centro CNR-ITC di Fisica degli Stati Aggregati (Trento) and the Università di Trento for hospitality and financial support. The financial support by ESRF (Project HS612-1998) is acknowledged.

Authors are grateful to the staff of the BM8-GILDA beamline for assistance during the measurements.

References

1. C. Armellini, M. Ferrari, M. Montagna, G. Pucker, C. Bernard, and A. Monteil, J. Non-Cryst. Solids **245**, 115 (2001).
2. C. Duverger, M. Montagna, R. Rolli, S. Ronchin, L. Zampedri, M. Fossi, S. Pelli, G.C. Righini, A. Monteil, C. Armellini, and M. Ferrari, J. Non-Cryst. Solids **280**, 261 (2001).
3. S. Sen and J.F. Stebbins, J. Non-Cryst. Solids **188**, 54 (1995).
4. B.T. Stone and K.L. Bray, J. Non-Cryst. Solids **197**, 136 (1996).
5. F. Rocca, G. Dalba, R. Grisenti, M. Bettinelli, F. Monti, and A. Kuzmin, J. Non-Cryst. Solids **233–234**, 581 (1998).
6. F. Rocca, A. Dalmaso, F. Monti, A. Kuzmin, and D. Pasqualini, J. Synchrotron Rad. **6**, 737 (1999).
7. F. Rocca, M. Ferrari, A. Kuzmin, N. Daldosso, C. Duverger, and F. Monti, J. Non-Cryst. Solids **293–295**, 112 (2001).
8. P.M. Peters and S.N. Houde-Walter, Appl. Phys. Lett. **70**, 541 (1997).
9. M. Braglia, G. Dai, S. Mosso, S. Pascarelli, F. Boscherini, and C. Lamberti, J. Appl. Phys. **83**, 5065 (1998).
10. F. d'Acapito, S. Mobilio, L. Santos, and R.M. Almeida, Appl. Phys. Lett. **78**, 2676 (2001).
11. F. d'Acapito, S. Mobilio, P. Bruno, D. Barbier, and J. Philipsen, J. Appl. Phys. **90**, 265 (2001).
12. N. Diab, G. Dalba, C. Armellini, F. Rocca, and C. Meneghini, in *Extended Abstracts of the XIX Intern. Congress on Glass* (Society of Glass Technology, Edinburgh, Scotland, 2001), p. 712.
13. A. Kuzmin, Physica B **208/209**, 175 (1995); A. Kuzmin, J. Physique IV 7, **C2-213** (1997).
14. A. Kuzmin and J. Purans, J. Phys.: Condensed Matter **12**, 1959 (2000).
15. J.J. Rehr, J. Mustre de Leon, S.I. Zabinsky, and R.C. Albers, J. Am. Chem. Soc. **113**, 5135 (1991); J. Mustre de Leon, J.J. Rehr, S.I. Zabinsky, and R.C. Albers, Phys. Rev. B **44**, 4146 (1991).